We are IntechOpen, the world's leading publisher of Open Access books Built by scientists, for scientists

4,800
Open access books available

122,000
International authors and editors

135M
Downloads

Our authors are among the

154
Countries delivered to

TOP 1%
most cited scientists

12.2%
Contributors from top 500 universities

CLARIVATE ANALYTICS BOOK CITATION INDEX INDEXED

WEB OF SCIENCE™

Selection of our books indexed in the Book Citation Index in Web of Science™ Core Collection (BKCI)

Interested in publishing with us?
Contact book.department@intechopen.com

Numbers displayed above are based on latest data collected.
For more information visit www.intechopen.com

21

A New On-Board Energy Storage System for the Rolling Stock

Masao Yano
Toyo University, Japan

1. Introduction

The increasing environmental problems, such as running out of fossil fuels, global warming, and pollution give a major impetus to the development of the on-board energy storage system for the rolling stock, using such as rechargeable batteries and electric double layer capacitors (EDLCs). In addition to the energy saving, an on-board energy storage system enables to realize a contact-wireless type railcar, by which the landscape is improved and the maintenance cost of overhead contact wires is reduced (Ogiwara, 2010).

Fig. 1. Typical commuter electric train in Japan

In case of the system with the catenary wire such as shown in Figure 1, the electrical regenerative braking has reduced total energy consumption in electric railway systems. However, if the energy is not absorbed by another train, the catenary voltage rises and regenerative failure is occurred under DC power feeding system. The train must be decelerated only with a mechanical brake. Therefore on-board energy storage system is a promising tool to prevent regenerative energy failure for rolling stock. As EDLCs have superiorities such as long lifetime and quick charge/discharge capability compared to rechargeable batteries, some systems using EDLC were designed and tested (Sekiyama et al., 2007), (Baklan, 2009), (Drabek & Streit, 2009).
Energy storage devices and their charge/discharge converters are shunt connected to main DC power source in the typical configuration as shown in Figure 2. In this configuration, the regeneration power is absorbed with EDLCs and braking is realized without other energy consuming trains. Figure 3 shows typical traction effort and power vs. speed characteristics in conventional traction systems using AC motors.

Costs and weights of energy storage devices are considerably large. If we fully use the ability of energy storage devices, the increased power and the traction effort can be realized both at powering and breaking. Prof. Sone et al. proposed two methods to realize increased power at high speed region (Sone et al., 2005). In this chapter, these two methods were investigated and compared in detail, and the increased voltage method was adopted preferably. Then the feasibility of the system was verified with simulations and experiments.

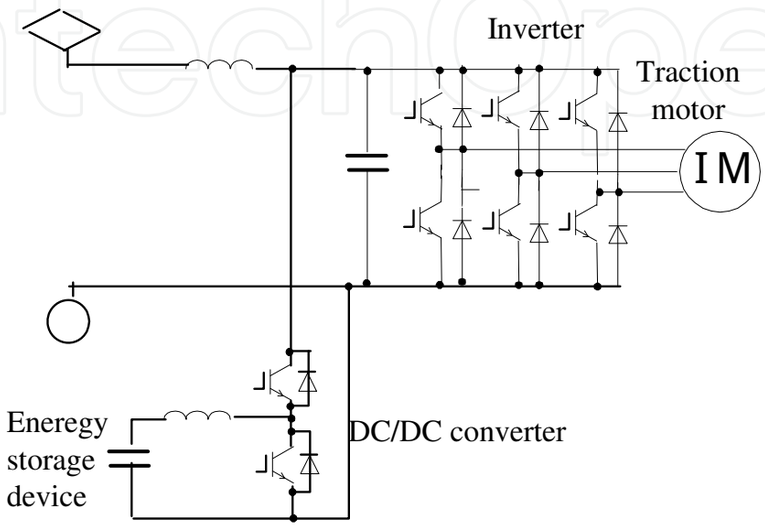

Fig. 2. Shunt connected energy storage device for DC electric rolling stock

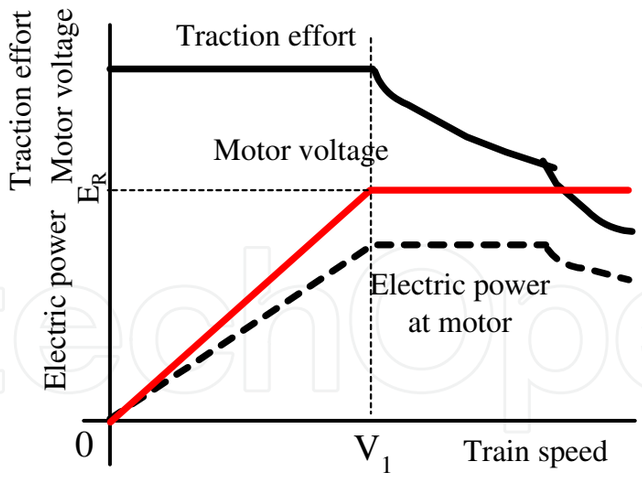

Fig. 3. Traction effort, power and voltage vs. speed characteristics in conventional systems

2. Increased power method at high speed region

Two methods were proposed to realize increased power at high speed region. One is the increased current method, in which the rated motor current is doubled and the motor rated voltage E_m is reduced to half at speed V_1 for example, and the motor voltage is increased to the maximum voltage E_R determined by the catenary voltage at the speed region over V_1 as

shown in Figure 4 (Abe et al. , 2006). The circuit configuration of this method is the same as that of the conventional method, shown in Figure 2.

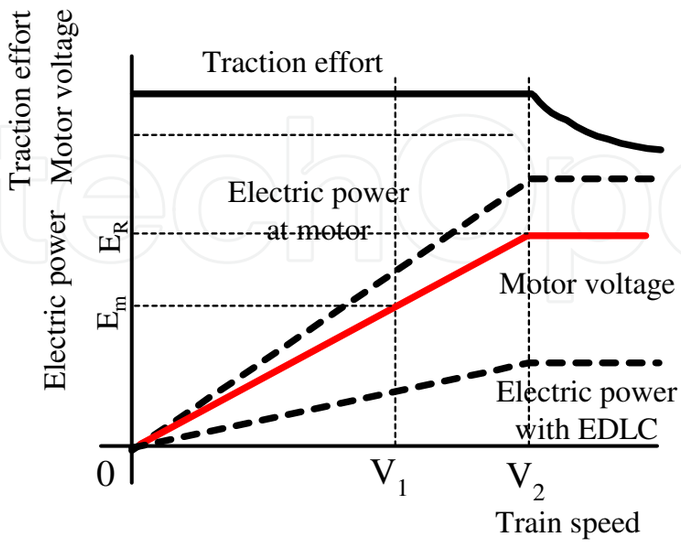

Fig. 4. Traction effort, power and voltage vs. speed characteristics in the system of increased current method

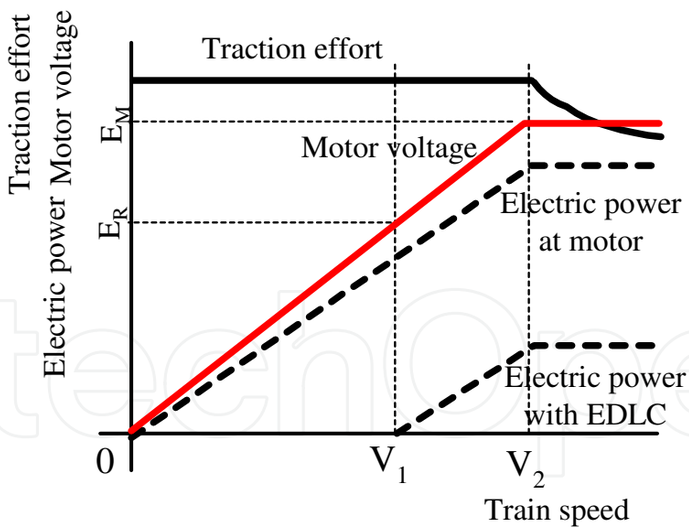

Fig. 5. Traction effort, power and voltage vs. speed characteristics in the system of increased voltage method

The other is the increased voltage method, in which the output voltage of the energy storage devices is added to the voltage generated by the overhead source at the speed region over V_1. The motor voltage is increased, and increased power and traction effort are realized both at powering and breaking as shown in Figure 5. In this system, increased power of the

traction motor is realized by increased voltage rather than increased current, and for DC side, increased power is fed from or stored to the energy storage devices, without increased catenary current. In the published papers (Yano et al., 2007), (Sone et al., 2005), a new system of increased voltage method using interface transformers between auxiliary inverters and motor windings was proposed. As we could dispense with these transformers with further studies, we developed the new energy storage systems, using EDLCs connected in series to main motor windings with such a simple circuit configuration as shown in Figure 6 (Yano et al., 2009).

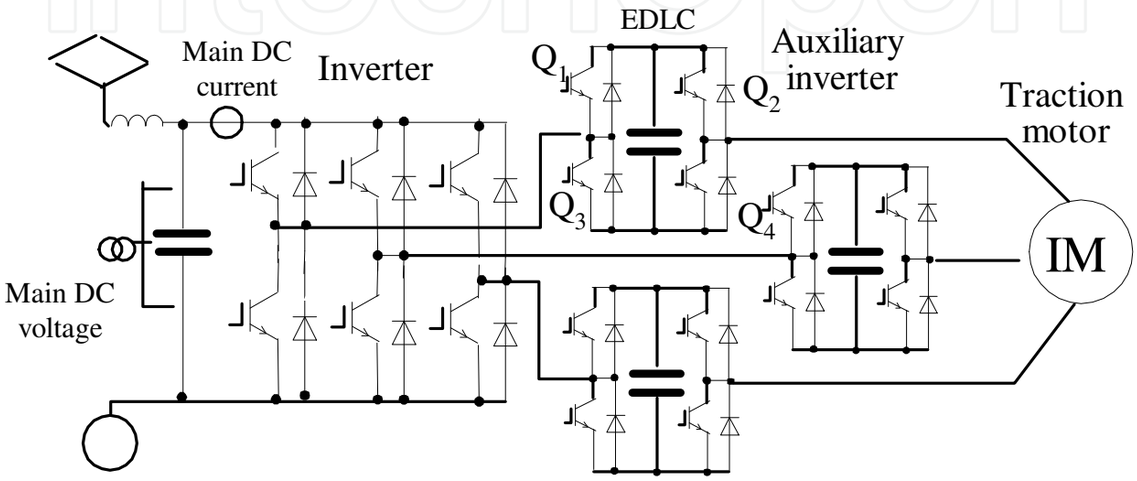

Fig. 6. Circuit configuration of energy storage system connected in series to main motor windings

3. System comparison

In the new systems of increased power with energy storage devices following the operating pattern shown in Figure 4 and Figure 5, the maximum speed V_2 of increased power depends on the output/input power of the DC/DC converter and the auxiliary inverter respectively. Thus the capacities of the DC/DC converter and the auxiliary inverter are selected, considering the desirable maximum speed V_2. For simple estimations, V_2 is selected to be twice V_1, and TABLE 1 shows evaluation results among three methods.

In the increased voltage method, the capacity of the auxiliary inverter is the same as the main inverter, and we can dispense with DC/DC converters which are required in the conventional method and the increased current method. In the current increased method, the motor of high current capacity is required. On the other hand, the power and the voltage of the traction motor are increased to be twice those in conventional systems in the voltage increased method. However the magnetic capacity of the motor (the product value by voltage and time) is the same value as that in the conventional method, and the physical scale of the motor does not increase considerably. For this reason, we prefer the voltage increased method rather than the current increased method.

	Conventional method	Increased current method	Increased voltage method
Traction effort at V_2	Half of rated torque	Rated torque	Rated torque
Traction motor	Rated voltage, rated current	Rated voltage, twice rated current	Twice rated voltage at V_2, rated current
Main inverter	Rated voltage, rated current	Rated voltage, twice rated current	Rated voltage, rated current
Auxiliary inverter	None	None	Rated voltage, rated current
EDLC charge circuit	Rated voltage, rated current	Rated voltage, rated current	None
System elements such as wires	Rated voltage, rated current	Rated voltage, twice rated Current	Twice rated voltage, rated current

Table 1. System comparison

4. Circuit configuration and control

The voltage increased method was adopted. The performance and feasibility are verified by simulation case studies and experiments under several conditions. For experiments, a 3 kVA inverter with the carrier frequency of 7 kHz, which consists of IGBTs, EDLCs, and the digital control system of dSpace's rt1103, was constructed and tested.

4.1 Circuit configuration

The basic configuration of the studied system is shown in Figure 6. In the regular mode, the output voltages of the auxiliary inverters (3 single-phase inverters) are added to the output voltage of the main inverter. In the bypass mode (Q_1 and Q_2:on, Q_3 and Q_4: off), the output voltages of the auxiliary inverters are kept zero, thus the traction motors are fed only with the main inverter.

In the experiments and simulations, an induction motor with ratings of 2.2 kW, 200 V, 9.4 A, 50 Hz and 1430 rpm was used, and 3 banks of 0.93 F EDLC were respectively used as energy storage devices of 3 phases. In each bank, 60 small cell capacitors (2.3 V, 56 F) were connected in series.

4.2 Control system

The basic block diagram of the main circuit and control is shown in Figure 7. A standard indirect coordinate-vector controller was adopted for the main PWM inverter (Yano & Iwahori, 2003), and the voltage command signal of the controller is used for the control of the auxiliary inverter as well. The output signal of the EDLC controller is multiplied with the voltage command signal of the vector controller and the share ratio of the burdens between the main inverter and auxiliary inverters is adjusted. Control circuits of initial charging of EDLC banks and voltage balancing among 3 EDLC banks were developed and implemented as well.

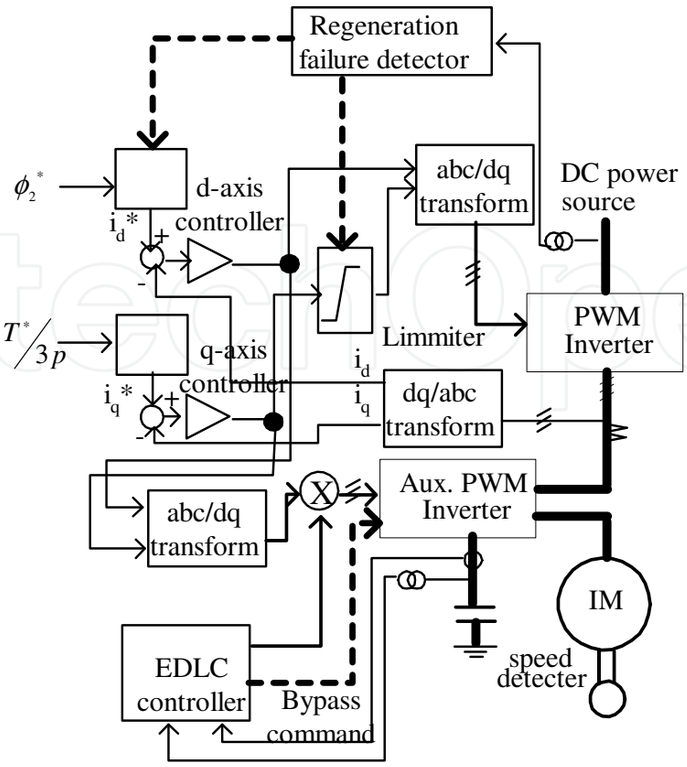

Fig. 7. Control block diagram

5. Simulation case study

Simulations using MATLAB/SIMULINK were carried out to prove the validity of the proposed method and to compare the method with conventional methods. The basic configuration of the studied system and system parameters are shown in Figure 6, and TABLE 2.

Main DC circuit voltage	300 V
Main IGBT inverter	3 kVA, carrier frequency= 7 kHz, operation frequency= 0 - 122 Hz
Auxiliary IGBT inverter	3 sets of 1 kVA, carrier frequency= 7 kHz, operation frequency= 0 - 122 Hz
EDLC	3 sets of 0.93 F, 60 cell capacitors connected in series
Induction motor ratings	2.2 kW, 200 V, 9.4 A, 50 Hz, 1430 rpm, rated d-axis current= 6.62 A, rated q-axis current= 10.5 A
Motor parameters	R_1= 0.881Ω, R_2= 0.658Ω, L_1= 0.815 H, L_2= 0.815 H, M= 0.0786 H
Inertia of the system	0.025 kg-m² at simulations, 28.9 kg-m² at experiments
Operations at conventional method	0 – 1430 rpm: constant-torque region, 1430 – 3000 rpm: constant-power region

Table 2. System parameters and motor data

5.1 Simulation results with conventional operating pattern

Figure 8 shows simulation results of the operation following the conventional operating pattern. At the speed weakening region over 1430 rpm, the d-axis current (magnetizing component) is reduced and the motor power is kept constant as 2.2 kW. The voltage of EDLC changes from 200 V to 199 V during discharging time with regular mode, and vice versa during charging time. Only the inertia of the motor is considered in simulations in order to reduce simulation time, and voltage changes of EDCLs are rather small.

Approximately 20 % - 40 % of the total power of the motor is shared by the storage devices. Traction effort vs. speed characteristics of this operation are the same as those of conventional trains, in which the regenerative power is absorbed by other trains through catenaries.

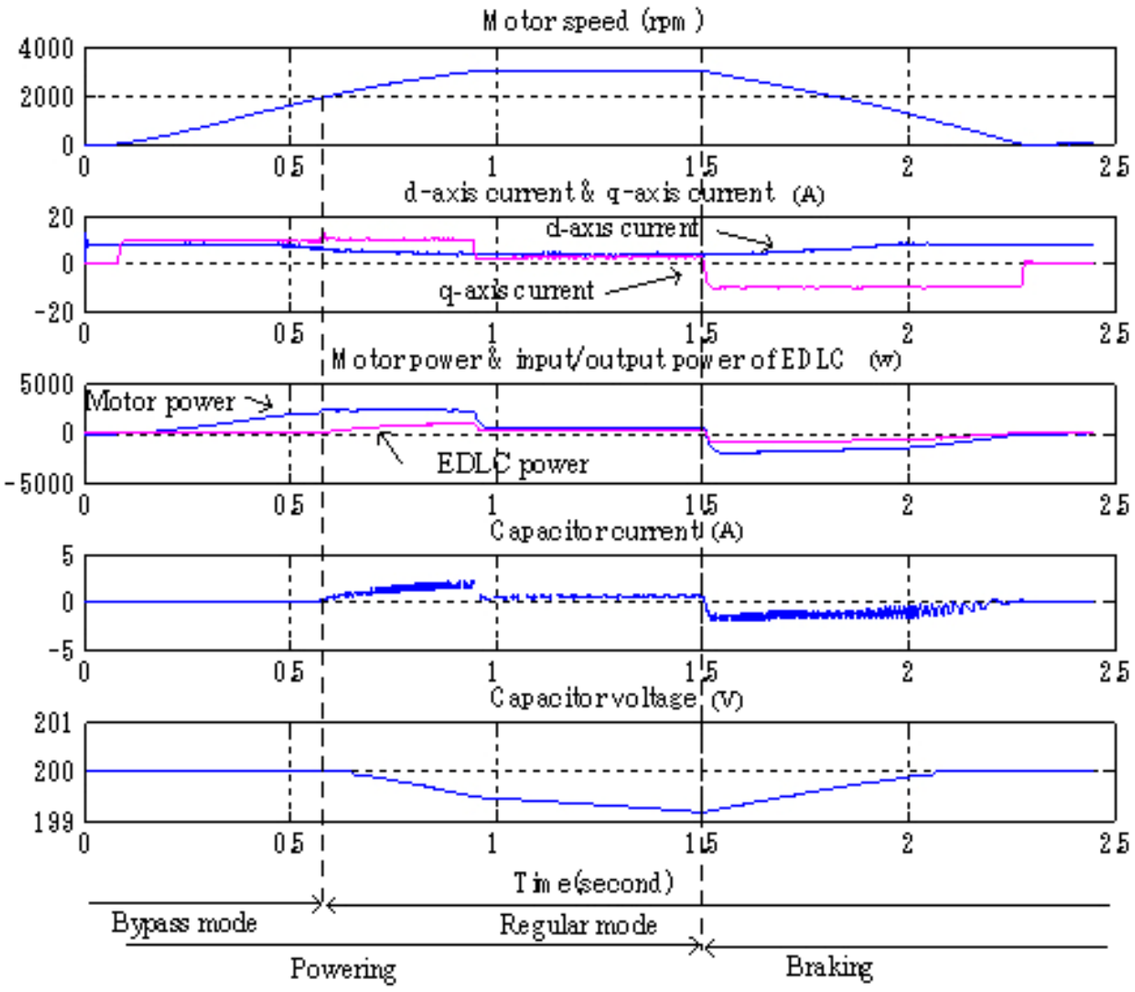

Fig. 8. Simulation wave forms at conventional operating pattern

5.2 Operation of regeneration failure at conventional operating pattern

Figure 9 shows operating results of regeneration failure at conventional operating pattern. Following the detection of regeneration failure due to the absence of other running trains, the regeneration power is only absorbed by on-board EDLCs. Although the regeneration power is reduced considerably, operations are maintained smoothly.

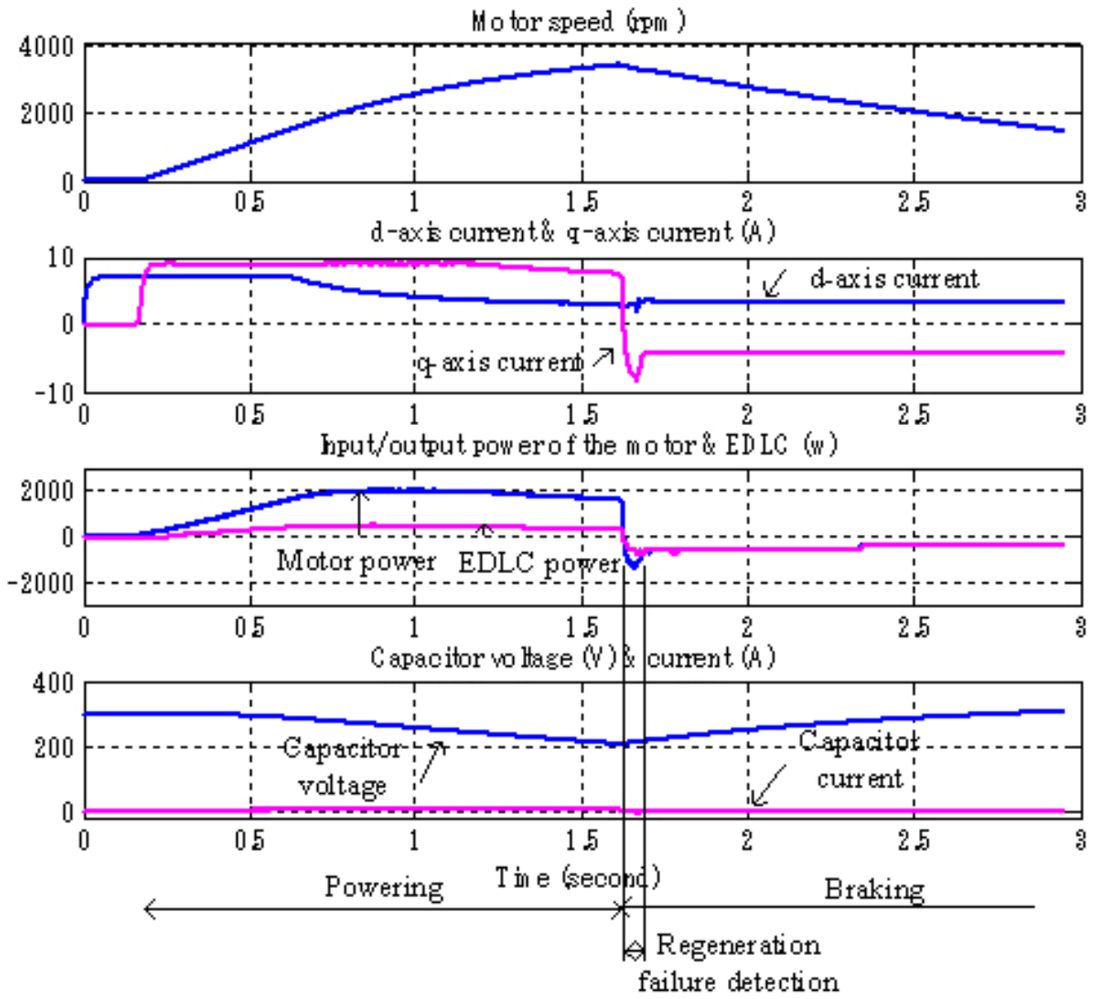

Fig. 9. Simulation wave forms at regeneration failure

5.3 Operation of increased power with energy storage devices

Figure 10 shows simulation results of the operation of increased power with energy storage devices. At all speed regions, the d-axis current (magnetizing component) is kept constant. At the speed region under 1430 rpm, the auxiliary inverter is at bypass mode, and plays no role in energy treatment. At the speed region over 1430 rpm, the auxiliary inverter is at regular mode, and shares the storage and the supply of the electric power, thus maximum motor power increases to 4.4 kW, twice that in conventional traction systems. The capacity of the auxiliary inverter is the same as that of the main inverter.

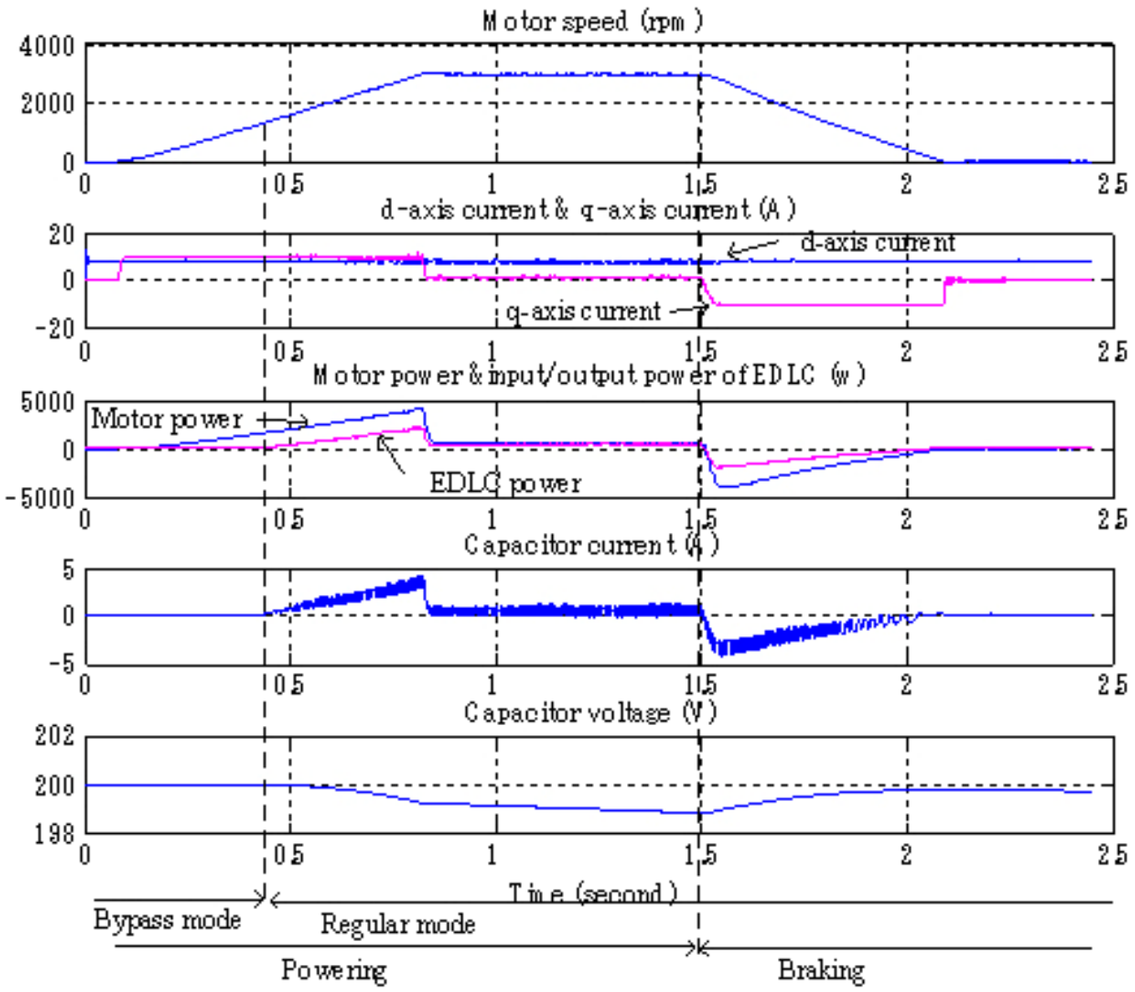

Fig. 10. Simulation wave forms in the new system of increased power with energy storage device

6. Experiments

The mini-model following the voltage increased method was constructed in the circuit configuration shown in Figure 6, and tested.

6.1 Experimental setup

A PWM inverter rated 3 kVA and auxiliary input/output systems for EDLCs, whose parameters are shown in TABLE 2, were designed and constructed. Figure 11 shows the outline of the mini model and the experimental setup. A flywheel shown in Fig. 12 was connected to the main motor to simulate the large inertia of the system. The flywheel, whose diameter and thickness are 50 cm and 30 cm respectively, was made with the iron steel and its inertia was 28.9 kg-m^2. Starting time from standstill to rated speed 1430 rpm is about 295 s. 3 sets of 0.93 F EDLC were respectively used as energy storage devices of 3 phases. In each set, 60 cell capacitors (2.3 V, 56 F) were connected in series.

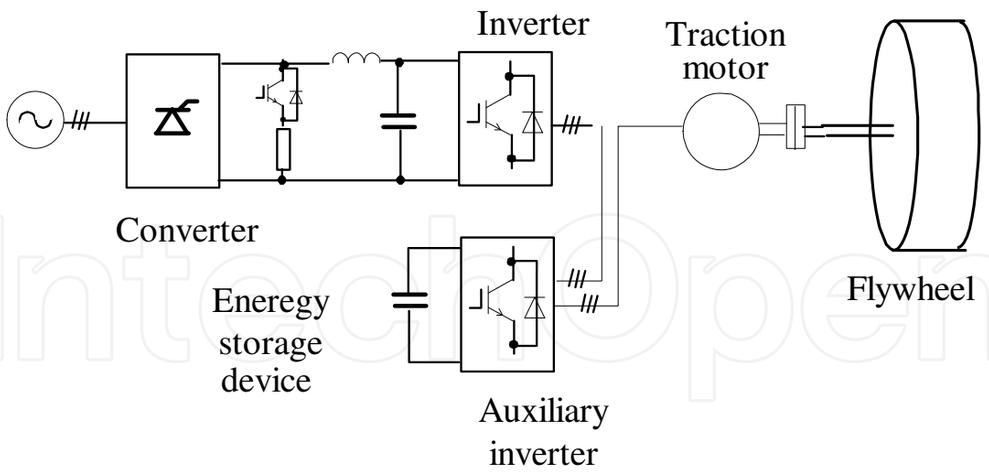

Fig. 11. Mini model and experimental setup

Fig. 12. Fly-wheel

6.2 Starting and low speed operation

Figure 13 shows experimental wave forms in starting from standstill to 40 rpm and braking from that speed to zero as shown as (d). The regular mode took place of the bypass mode about 3 s after starting, but motor currents (c) kept regular sinusoidal wave forms and no transient effects were observed. Torque current (q-axis current) (e) was kept 10.5 A during mode change, and changed to -10.5 A at braking. Magnetizing current (d-axis current) was also observed to be constant during whole operation.

At the mode change, main DC circuit current (b) began to decrease, and discharging current of EDLC (g) began to flow. As EDLCs were divided among each phase, EDLC current showed ripple of twice operating frequency. EDLC voltage (f) decreased due to discharging, but EDLC was not charged significantly during braking, as the regenerative energy was small at low speed operation.

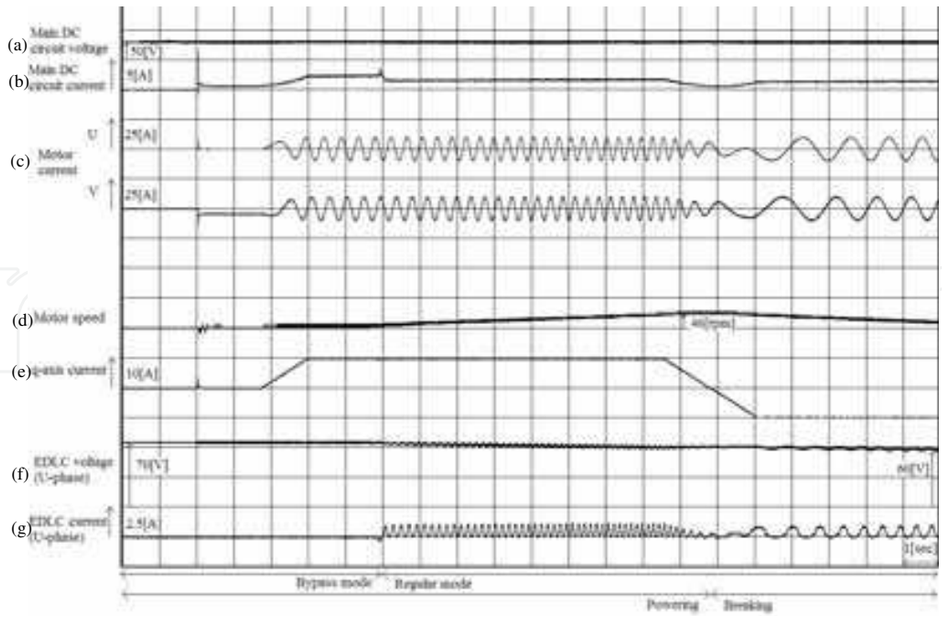

Fig. 13. Experimental wave forms in starting and low speed operation

6.3 Normal speed operation

Fig. 14 shows experimental waveforms at normal speed operation. The bypass mode was changed to the regular mode at the speed of 460 rpm during acceleration with rated torque, and the regenerative braking was added at the speed of 500 rpm. At the mode change, main DC circuit current (b) began to decrease, and the discharging current of EDLC (g) began to flow. EDLC voltage (f) decreased to 47 V from 70 V. Q-axis current of the motor (e) was kept constant, and was shared with the main inverter and the auxiliary inverters. After several seconds, torque command was changed from powering to braking, and EDLC was charged with braking power, thus its voltage increased from 47 V to 85 V. Charge/discharge power was about 200 W and total discharge energy was 3800 J. All operations including starting transients were smooth as expected.

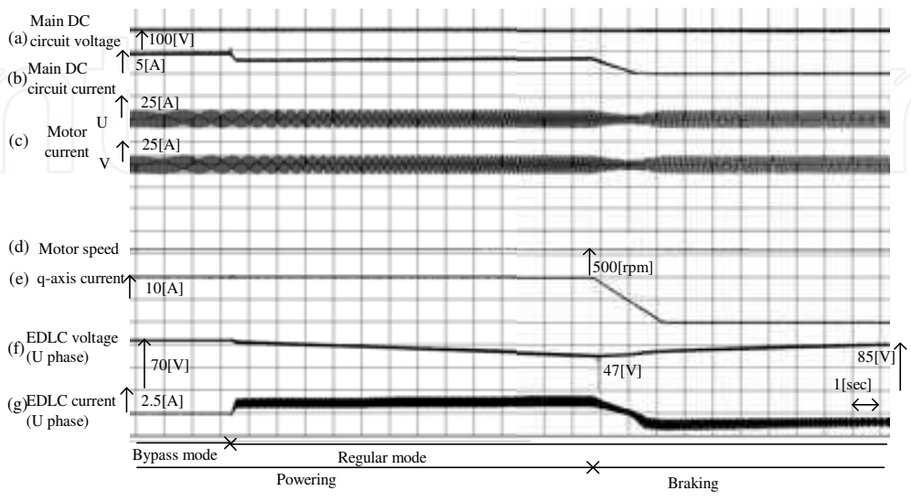

Fig. 14. Experimental wave forms in normal speed operation of the new system

6.4 Initial charging and voltage balancing of EDLC

At the first stage of operations, three banks of EDLC are individually charged in the proper order with the main inverter. In charging of U-phase EDLC, all arms of U-phase auxiliary inverter are off and the inverter works as a rectifier. The other two auxiliary inverters are at bypass mode, thus work as short circuits. Reference signals of output voltages of V-phase and W-phase of the main inverter are kept zero and the charging current is controlled by two U-phase arms of the main inverter. Experimental wave forms in Figure 15 shows that each bank of EDLC was charged with constant current smoothly.

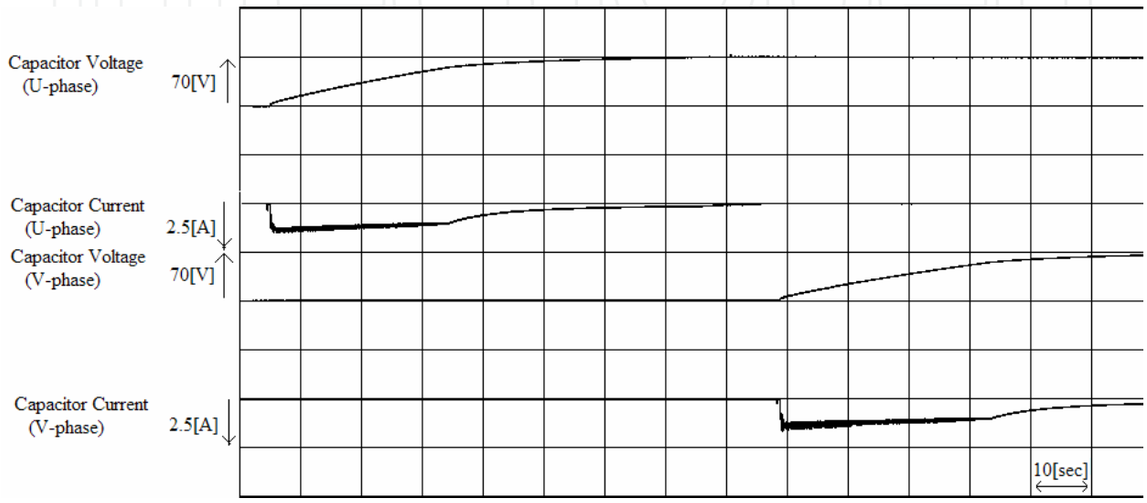

Fig. 15. Experimental results of initial charge operation

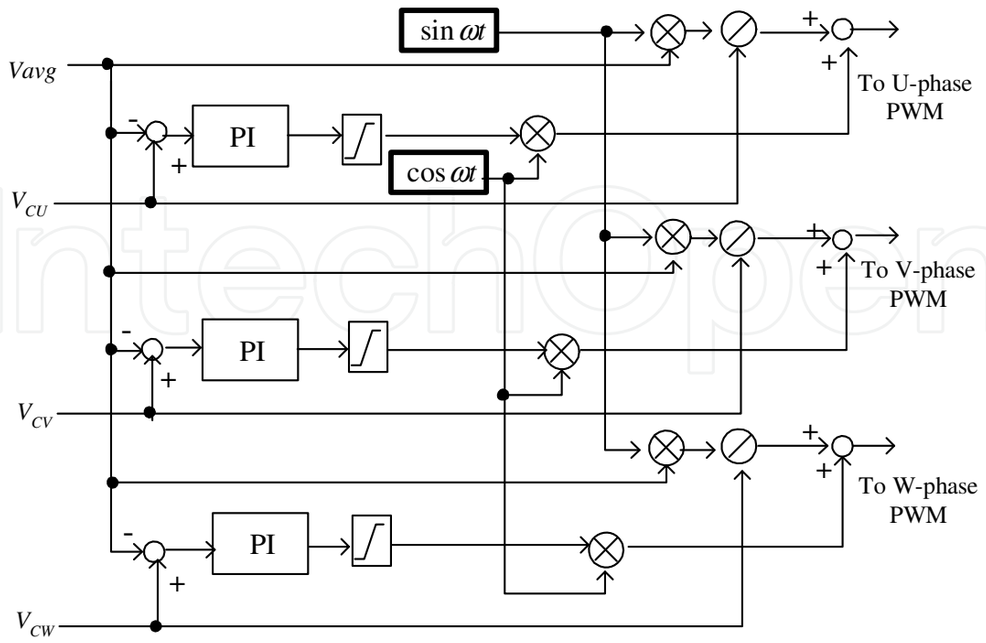

Fig. 16. Block diagram of balancing control

Balancing control of EDLC voltages among three banks takes place both after the initial charging and at the standstill operation. The output voltage of the main inverter is kept to zero and only auxiliary inverters work to equalize three voltages of EDLC banks. Figure 16 shows block diagram of balancing control. Three auxiliary inverters generate three alternative voltage of 50 Hz. Amplitudes of the direct component of the voltage ($\sin \omega t$) are controlled to be the same among three outputs and the quadratic components of the voltage ($\cos \omega t$) are added depending on the difference between EDLC voltage of each phase (V_{CU}, V_{CV}, V_{CW}) and the average value among three banks (V_{avg}). The phase angle of the output voltage for the EDLC bank of higher voltage leads those of other voltages, and energy flows from this bank to other banks, so that EDLC voltages are equalized among three banks. Figure 17 shows experimental results of balancing control. Leading or lagging phase angles were limited to 8°, and currents of charging and discharging were kept within constant values, thus smooth charging and discharging were observed.

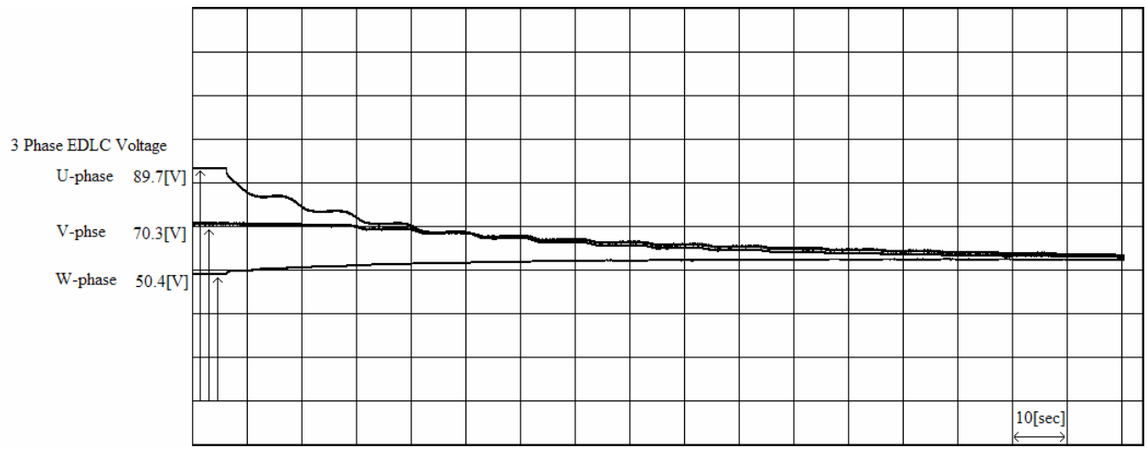

Fig. 17. Experimental results of balancing control

7. Capacity estimation of EDLC

The selection of the capacity of energy storage device depends on many factors such as railway conditions, traction efforts of rolling stock, the setting of desirable maximum power, and so on. Some specifications of on-board energy storage devices were shown in materials (Takahara & Wakasa, 2002), (Technical committee of IEEJ, 2004). Hereafter some estimates are presented referring these materials.

At a standard Japanese commuter 1M1T electric train of 65 t weight including passengers m, 80 % of moving energy is assumed to be charged as electric energy, and the electric energy Q is calculated as follows.

At rated speed of 70 km/h (=19.4 m/s) $v_{\mathbf{rated}}$,

$$Q_{\mathbf{rated}} = 0.8\text{x}0.5\text{x}m{v_{\mathbf{rated}}}^2 = 0.8\text{x}0.5\text{x}65\text{x}10^3\,\text{x}19.4^2 = 10\,\left[\text{MJ}\right] = 2.78\,\left[\text{kWh}\right]. \quad (1)$$

At top speed of 100 km/h (=27.8 m/s) $v_{\mathbf{top}}$,

$$Q_{\mathbf{top}} = 0.8\text{x}0.5\text{x}m{v_{\mathbf{top}}}^2 = 0.8\text{x}0.5\text{x}65\text{x}10^3\,\text{x}27.8^2 = 20\,\left[\text{MJ}\right] = 5.56\,\left[\text{kWh}\right]. \quad (2)$$

The energy difference between Q_{top} and Q_{rated} is 10 [MJ]. Figure 18 shows simplified power share of EDLC referring to total motor power. This indicates that rated traction or braking effort can be realized at the top speed, if around a quarter of this energy (2.5 [MJ]), is charged /discharged with on board EDLC. This train is driven with 4 motors of 150 kW, and the catenary voltage is DC 1.5 kV.
At top speed, total traction/braking power is 857 kW(=4x150x100/70) and it corresponds to DC power of 400 A and 2142 V.
Charge energy of 2.5 F EDLC from 1.15 kV to 1.85 kV Q_{cap}, is calculated as follows and meets the requirement.

$$Q_{cap} = 0.5\text{x}2.5\text{x}\left(\left(1.85\text{x}10^3\right)^2 - \left(1.15\text{x}10^3\right)^2\right) = 2.63\ [\text{MJ}] \tag{3}$$

Figure 19 shows the picture of a EDLC case unit of 160 V, 3.7 F and 50 A, and one case unit houses 70 EDLC cells (Meidensya, 2009). Using these case units, 3 sets of 0.85 F, 2.0 kV EDLC can be constructed with 117 case units. 1 set consists of 3 parallel circuits of 13 case units in series. Total estimated weight of EDLC is around 1 t.
The traction effort F can be calculated as follows.

$$F = (1/9.8)\text{x}P_{\text{rated}} / v_{\text{rated}} = (1/9.8)\text{x}600/19.4 = 3160\ [\text{kg} - \text{weight}] \tag{4}$$

If the equivalent weight of rotation inertia is assumed to be 9% of total weight m, and the travelling resistance of the train is neglected, the acceleration/deceleration rate α can be calculated as follows.

$$\alpha = 3.6\text{X}9.8F / \left(1.09\text{x}m\text{x}10^3\right) = F / (31\text{x}m) = 1.57\ [\text{km/h/s}] \tag{5}$$

$$\alpha = 3.6\text{X}9.8F / \left(1.09\text{x}m\text{x}10^3\right) = F / (31\text{x}m) = 1.57\ [\text{km/h/s}] \tag{5}$$

This traction effort and the acceleration/deceleration rate can be realized through all operations. However the friction brake must be used additionally with this installation, when receptive conditions of the catenary are insufficient or lost.

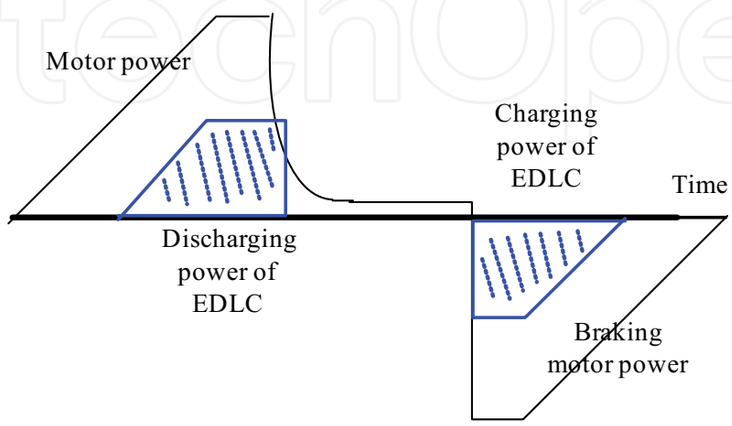

Fig. 18. Total motor power & charging/discharging power of EDLC

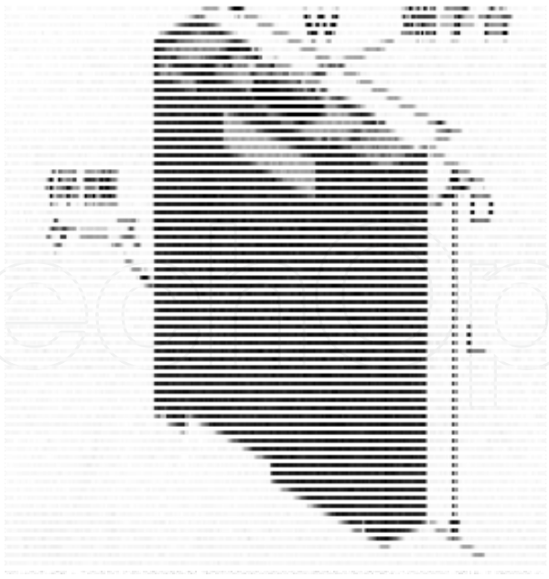

Fig. 19. EDLC case unit-160 V, 3.7 F, 50 A, 8.8 kg, W: 272 mm, L: 387 mm, D: 51 mm

8. Conclusion

A new configuration of an energy storage system, consisting of EDLCs and their input-output auxiliary inverters connected in series to main motor windings was presented, and the superiority of this system was verified by simulation case studies and experiments. This configuration can increase maximum traction and regeneration power substantially without increasing the motor current and the catenary current. Wide assessment, which includes the setting of desirable maximum power, the selection of the capacity of energy storage device, and estimates for cost, weight and size, must be carried out for specified rolling stock. As a result, the adoption of this system to actual electric rolling stock is expected.

9. Acknowledgment

This work has been supported by the Faulty of Engineering, Toyo University, in Japan.

10. References

Abe, T. ; Sone, S. ; Takano, S. et al. (2006). A Study of Improved Regeneration over High-Speed Region by Increased Current Method and Verification by Model Experiment, *IEEJAnnual Conference 2006*, pp. 5-213-214

Baklan, Mark-M. (2009). A Power Electronics View on Rail Transportation Applications, *Proceedings of EPE 2009*, ISBN 978-907-5815-009, Barcelona, Spain, October, 2009

Drabek, P. & Streit, T. (2009). The Energy Storage System for Public Transport Vehicles, *Proceedings of EPE 2009*, ISBN 978-907-5815-009, Barcelona, Spain, October, 2009

Meidensya (2009). MEICAP specification, *Meidenjiho* Vol.1, 2009, p 7

Ogihara, T. (2010). Chapter 6 :Development of contact-wireless type railcar by lithium ion battery, In:*Electric Energy Storage*, InTech, ISBN 978-953-307-058-2

Sekijima, Y.; Inui, M.; Aoyama, I. & Monden, Y. (2007). A trial of regenerated energy storage with an electric double layer capacitor for rolling stock, *IEEJ-IAS Annual Conference 2007*, 1-05-5, pp. I-125-128

Sone, S.; Satoh, T. & Kamiyama, J. (2005). Proposal and Discussion of High-Speed Regenerative Braking – For Realizing Genuine Pure Electric Braking, *The Papers of Technical Meeting on Transportation and Electric Railway*, *IEEJ*, TER-05-26, pp. 71-74, 2005

Takahara, E. & Wakasa, T. (2002). Electric Double Layer Capacitors for Electric Railway Vehicles, *The Papers of Technical Meeting on Transportation and Electric Railway*, *IEEJ*, TER-02-33, pp. 27-30, 2002

Technical committee of IEEJ (2004). Power Electronics Applications in Railways, *IEEJ Technical Report*, No. 979, ISSN0919-9195, pp. 64-66

Yano, M. ; Kurihara, M. & Kuramochi, S. (2009). A New On-board Energy Storage System for the Railways Rolling Stock Utilizing the Overvoltage Durability of Traction Motors, *Proceedings of EPE 2009*, ISBN 978-907-5815-009, Barcelona, Spain, October, 2009

Yano, M.; Mizumura, T. & Kuramochi, S. (2007). A New Energy Storage System for Railway Rolling Stock Using Transformers Connected in Series to Motor Windings, *Proceedings of The IEEE International Electric Machines and Drives Conference*, pp. 112-117, Antalya, Turkey, May, 2007

Yano, M. & Iwahori, M. (2003). Transition from Slip-Frequency Control to Vector Control for Induction Motor Drives for Traction Application in Japan, *Proceedings of the IEEE International Conference on Power Electronics and Drive Systems*, pp. 1246-1251, Singapore, November, 2003

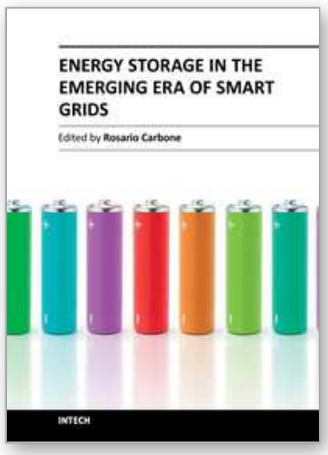

Energy Storage in the Emerging Era of Smart Grids

Edited by Prof. Rosario Carbone

ISBN 978-953-307-269-2
Hard cover, 478 pages
Publisher InTech
Published online 22, September, 2011
Published in print edition September, 2011

Reliable, high-efficient and cost-effective energy storage systems can undoubtedly play a crucial role for a large-scale integration on power systems of the emerging â€œdistributed generationâ€ (DG) and for enabling the starting and the consolidation of the new era of so called smart-grids. A non exhaustive list of benefits of the energy storage properly located on modern power systems with DG could be as follows: it can increase voltage control, frequency control and stability of power systems, it can reduce outages, it can allow the reduction of spinning reserves to meet peak power demands, it can reduce congestion on the transmission and distributions grids, it can release the stored energy when energy is most needed and expensive, it can improve power quality or service reliability for customers with high value processes or critical operations and so on. The main goal of the book is to give a date overview on: (I) basic and well proven energy storage systems, (II) recent advances on technologies for improving the effectiveness of energy storage devices, (III) practical applications of energy storage, in the emerging era of smart grids.

How to reference

In order to correctly reference this scholarly work, feel free to copy and paste the following:

Masao Yano (2011). A New On-Board Energy Storage System for the Rolling Stock, Energy Storage in the Emerging Era of Smart Grids, Prof. Rosario Carbone (Ed.), ISBN: 978-953-307-269-2, InTech, Available from: http://www.intechopen.com/books/energy-storage-in-the-emerging-era-of-smart-grids/a-new-on-board-energy-storage-system-for-the-rolling-stock

INTECH
open science | open minds

InTech Europe
University Campus STeP Ri
Slavka Krautzeka 83/A
51000 Rijeka, Croatia
Phone: +385 (51) 770 447
Fax: +385 (51) 686 166
www.intechopen.com

InTech China
Unit 405, Office Block, Hotel Equatorial Shanghai
No.65, Yan An Road (West), Shanghai, 200040, China
中国上海市延安西路65号上海国际贵都大饭店办公楼405单元
Phone: +86-21-62489820
Fax: +86-21-62489821

IntechOpen